

Poly(vinyl amine)—Silica Composite Nanoparticles: Models of the Silicic Acid Cytoplasmic Pool and as a Silica Precursor for Composite Materials Formation

Vadim V. Annenkov,^{*,†} Elena N. Danilovtseva,[†] Victor A. Pal'shin,[†] Vladimir O. Aseyev,[‡] Alexander K. Petrov,[§] Alexander S. Kozlov,[§] Siddharth V. Patwardhan,^{||} and Carole C. Perry^{||}

[†]Limnological Institute SB RAS, 3, Ulan-Bator Str., Irkutsk, 664033, Russia

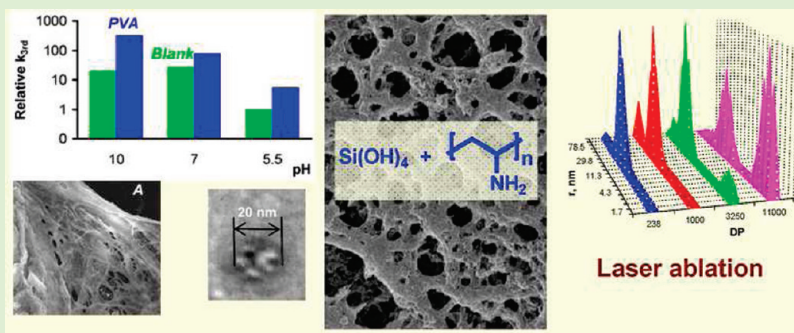
[‡]Laboratory of Polymer Chemistry, Department of Chemistry, University of Helsinki, P.O. Box 55, 00014 HY Helsinki, Finland

[§]Institute of Chemical Kinetics and Combustion, Institutskaya 3, Novosibirsk, 630090, Russia

^{||}Nottingham Trent University, Clifton Lane, Nottingham, NG11 8NS Great Britain

S Supporting Information

ABSTRACT:



The role of polymer (poly(vinylamine)) size (238–11000 units) on silicic acid condensation to yield soluble nanoparticles or composite precipitates has been explored by a combination of light scattering (static and dynamic), laser ablation combined with aerosol spectrometry, IR spectroscopy, and electron microscopy. Soluble nanoparticles or composite precipitates are formed according to the degree of polymerization of the organic polymer and pH. Nanoparticles prepared in the presence of the highest molecular weight polymers have core–shell like structures with dense silica cores. Composite particles formed in the presence of polymers with extent of polymerization below 1000 consist of associates of several polymer–silica nanoparticles. The mechanism of stabilization of the “soluble” silica particles in the tens of nanometer size range involves cooperative interactions with the polymer chains which varies according to chain length and pH. An example of the use of such polymer–poly(silicic acid) nanoparticles in the generation of composite polymeric materials is presented. The results obtained have relevance to the biomimetic design of new composite materials based on silica and polymers and to increasing our understanding of how silica may be manipulated (stored) in the biological environment prior to the formation of stable mineralized structures. We suspect that a similar method of storing silicic acid in an active state is used in silicifying organisms, at least in diatom algae.

INTRODUCTION

Over the past decade, silicifying organisms such as diatom algae, sponges, and some plants (horsetail, rice) have become a focus of attention for biologists, chemists, and related specialists, including nanotechnologists. The reasons for this are the large ecological and economic significance of these organisms, a desire to understand the molecular mechanisms of biosilicification and the potential practicality of this knowledge. One of the insufficiently studied stages in silica accumulation by living organisms is the cytoplasmic form of silicon. In our opinion, however, this process is the most investigated for diatoms. Until recently, various silicon compounds were discussed: free silicic acid,¹ organo-silicon compounds,² solid

silica nanoparticles,^{3,4} and stabilized oligomers of silicic acid.^{5–7} The study of diatom biomass with solid-state NMR^{8,9} revealed only condensed Si(OH)_4 in the cells and the absence of electron-dense silica particles in cytoplasm¹⁰ reduces the possible forms of silicon present to oligosilicates, but it is not known how these are formed and regulated.

Studies of diatoms has led to the discovery of special proteins—silaffins that are associated with biosilica.^{6,11–13} These proteins

Received: January 31, 2011

Revised: April 7, 2011

Published: April 07, 2011

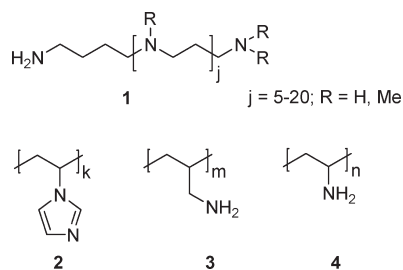


Figure 1. Structures of biogenic polyamines (1),^{6,12,14} PVI (2), polyallylamine (3), and PVA (4).

contain polyamine side chains with up to 20 nitrogen atoms, and free polyamines were also found in some diatoms.^{6,12,14,15} The physiological function of silaffins is not fully known or understood, the initial suggestion being that these compounds function as the matrix in the biosynthesis of ordered silica structures, for example, diatom exoskeletons.^{6,12,16} This hypothesis is not confirmed *in vivo*, but these results stimulated studies of silicic acid condensation in the presence of polymeric bases and ampholytes.

In particular, it was found^{6,7,17} that primary nanoparticles of poly(silicic acid) can be stabilized in solution by complexing with amino- or imidazole-containing polymers. In the case of poly(1-vinylimidazole) (PVI), the interaction between imidazole units and silanol groups decreases the activity of $\equiv\text{Si}-\text{OH}$ in further condensation.⁷ This interaction results in composite precipitates or in stable nanoparticles, depending on the extent of polymerization of PVI: long chains are able to stabilize particles in solution, and the short macromolecules link silica nanoparticles to one another. In both cases, formation of hydrogen bonds between silanol groups and imidazole groups inhibits further condensation due to a reduction in availability of $\equiv\text{Si}-\text{O}^-$ anions that are active in nucleophilic reaction with monomeric $\text{Si}(\text{OH})_4$. Condensation of silicic acid in the presence of poly(allylamine) results⁶ in stable soluble nanoparticles about 40–60 nm in diameter, and this observation is the closest model of the biogenic polyamine– $\text{Si}(\text{OH})_4$ system. Unfortunately, allylamine is a poorly polymerizable monomer and the corresponding polymer is available as low molecular weight samples only.

Poly(vinylamine) (PVA), however, is a more convenient and structurally relevant polymer to study the influence of polymeric amines on silicic acid condensation in water. Figure 1 shows a comparison of biogenic polyamine structures and those of PVI, polyallylamine, and PVA. PVA can be readily synthesized from poly(vinyl formamide) (PVFA), which is available in the form of narrow molecular weight fractions.¹⁶

In this study we have prepared PVA samples of various degree of polymerization (DP, 238–11000 units) and studied their influence on the condensation of silicic acid using a combination of light scattering (dynamic and static) methods (DLS and SLS), laser ablation using a free electron laser (FEL) in the terahertz region combined with aerosol spectrometry, FTIR spectroscopy, and electron microscopy. The application of laser ablation using a free electron laser is a novel application in this area of research but it has recently been shown¹⁹ that under the action of submillimeter (120–240 μm) radiation from FEL, nanoparticles can be gently transferred from solution or solid phases to the aerosol state and their size and quantity measured with modern aerosol equipment. The advantage of ablation with FEL consists in correspondence between laser frequencies (40–80 cm^{-1}) and vibrations of hydrogen bonds, and so destruction of covalent

bonds is unlikely. The softness of the ablation technique has been confirmed by the retention of enzymatic activity of horseradish peroxidase and PCR-proven integrity of lambda phage DNA, plasmid pUC18DNA after all manipulations.¹⁹ The technique was investigated for its ability to provide complementary information to that obtained by light scattering, which suffers from the problem that the data obtained are all cumulative and results obtained from complex systems of particles of a different nature must be treated with caution.

Using the range of experimental methods listed above, we have obtained and characterized organo-silica nanoparticles based on PVA and suggest they may be potential building blocks for the design of more complicated nanocomposites. In addition, the results obtained reinforce the hypothesis concerning silicon transport vesicles as complexes between organic polymers and oligosilicates.^{7,20}

EXPERIMENTAL SECTION

Ethanol, dioxane, NaOH, $\text{Na}_2\text{SiO}_3 \cdot 5\text{H}_2\text{O}$, 1 M HCl solutions, and reagents for the molybdenum blue assay (ammonium molybdate, oxalic acid, 4-methylaminophenol sulfate, sodium sulphite, standard silicate solution, hydrochloric acid (35%), and sulphuric acid (98%)) were purchased from Sigma Aldrich, Fisher, or Acros chemicals and used without further treatment. Vinylformamide, 1-vinylimidazole, and acrylic acid (Sigma Aldrich) were purified from stabilizers by vacuum distillation before use. 2,2-Azobis(isobutyronitrile) (Sigma Aldrich) was crystallized from ethanol.

PVA was obtained by alkaline hydrolysis of PVFA.²¹ PVFA was synthesized by radical polymerization of vinylformamide in ethanol (10% solution) under the action of 2,2-azobis(isobutyronitrile) (2% from the monomer mass) at 60 °C for 6 h under an argon atmosphere. The obtained precipitate was washed with ethanol and dried under vacuum. Yield: 92%. PVFA was fractionated by precipitation from 1.5% water solution into dioxane. DP of PVFA fractions was measured by viscometry using constants from.¹⁸ VI-AA copolymers were synthesized according to ref 20 by radical polymerization in water. Polymer concentration is presented with respect to the repeating unit everywhere in the article.

Sodium silicate (10 mM) was used as a precursor of $\text{Si}(\text{OH})_4$ in this study. The desired pH was adjusted with 1 M HCl over 30–60 s using predetermined volumes of the acid. Concentration of orthosilicic acid was measured by the molybdenum blue colorimetric method.^{23,24} This method is based on the formation of a silicic acid – molybdate complex followed by reduction with ‘metol’ and measurement by colorimetry at 810 nm. The reaction conditions chosen only allow the interaction of monomers and dimers of silicic acid with the molybdate reagent without hydrolysis of more condensed species. A total of 3–5 specimens were taken for each point, and the relative standard deviation was below 5%. Kinetic data on silicic acid condensation were processed using a plot of $1/[\text{Si}(\text{OH})_4]^2$ versus time, which gives a straight line for the first 30–60 min of reaction, in accordance with third order kinetics being obeyed with the rate constant (k_{third}) being obtained from the gradient of the plot.²² The kinetic experiments were repeated three times, giving <10% experimental error in the calculated k_{third} . Composite precipitates were collected by centrifugation (3000 g, 5 min), twice washed with cold water (2–4 °C), and freeze-dried.

Zeta-potential (ζ) and time dependence of R_h were measured with a Zetasizer Nano-ZS ZEN3600 (Malvern Instruments Ltd, U.K.), equipped with a 4 mW He–Ne laser operating at $\lambda_o = 633$ nm. Measurements of zeta-potential were performed at $\theta = 17^\circ$. Simultaneously, R_h was determined at the back scattering angle of $\theta = 173^\circ$. Size and zeta-potential-DTS1060 folded capillary cells were employed for the simultaneous R_h and ζ measurements. Calculation of ζ values was performed using software supplied with the Zetasizer. Temperature was stabilized with a Peltier temperature control.

Table 1. SLS and DLS of PVA Fractions (in 0.2 M HCl and 0.1 M NaCl)

DP	MW, g/mol (DP) from SLS	r_g^a	r_h^a (% of the peak intensity)
238	22700 (528)	14.6	4.4 (86); 131 (14)
1000	113000 (2630)	20.4	5.8 (66); 165 (34)
3250	235000 (5470)	25.3	8.6 (70); 85.8 (30)
11000	437000 (10160)	42.2	37.1

^a r_g , radius of gyration (SLS); r_h , hydrodynamic radius (DLS, 30°, 488 nm scattering).

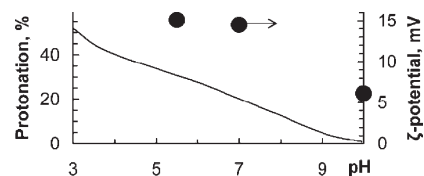
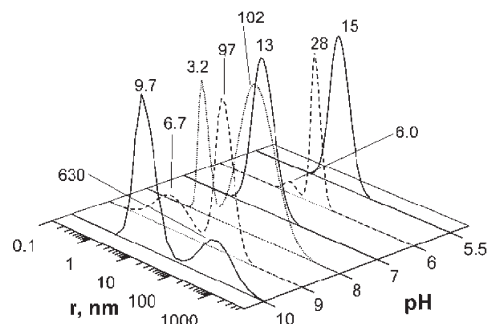
Multiangle SLS and DLS experiments (including DLS data in Table 1) were performed using a Brookhaven Instruments BI-200SM goniometer, a BIC-TurboCorr digital pseudocross-correlator, a BI-CrossCorr detector including two BIC-DS1 detectors, a Sapphire 488–100 CDRH laser from Coherent GmbH operating at $\lambda_o = 488$ nm and the power adjusted in the range from 10 to 50 mW was used as the light source. Scattered light was collected in the angular range between 30° and 150°. Correlation functions in DLS were analyzed using a model of log-normal distributed relaxation times and presented as intensity vs hydrodynamic radius. Examples of the experimental data and calculated values are presented in Supporting Information. All LS measurements were performed at 20 °C. Each particle size measurement was repeated 5–10 times, with the objective to minimize fluctuations in scattering intensity (SLS) and to increase reliability of the mathematical procedures in DLS.

IR spectra were recorded with an Infracum FT-801 spectrometer using KBr pellets using identical weights of the materials formed. Scanning electron microscopy (SEM) was performed using JEOL JSM-840A and FEI Quanta 200 instruments. The samples were placed on double-sided sticky carbon tape mounted on aluminum sample holders and then sputter-coated with gold using a SDC 004 (BALZERS) device. The coating settings (working distance 50 mm, current 15 mA, time 75 s) correspond to 12 nm gold coating according to the device manual. Transmission electron microscopy (TEM) was performed using a Philips EM 420 instrument on freeze-dried solutions 10-fold diluted just before freezing. The solid products were dispersed in hexane and drops of the solution place on Formvar film coated copper grids.

To study the samples by submillimeter laser ablation, the aqueous solutions were freeze-dried on a substrate made from aluminum foil. After that, the sample was placed into a horizontal cell into which filtered gaseous nitrogen was admitted in excess to prevent the arrival of aerosols from outside the cell. Before making measurements, the absence of aerosols in the whole air line was tested and confirmed. In the present study, an automatic diffusion battery with a condensation particle counter²⁵ was used to determine the particle size distribution of ablation products within the size range 3–250 nm; the source of the terahertz radiation was the free electron laser of the Siberian Center for Photochemical Research,²⁶ the laser wavelength was 128–131 μm . The power density necessary for the start of ablation was established by moving the sample along the focal axis of the sector mirror with the focal distance $f = 10$ cm; its average value was 20 W/cm². The resulting aerosol was carried by flowing nitrogen into a buffer reservoir 25 L in volume to stabilize the number concentration of particles. Then the aerosol was brought to the diffusion aerosol spectrometer to analyze the particle size distribution. Time of a single measurement was 4 min. Measurements were carried out in series of four measurements in each series, with the size distributions being averaged over the series. Irradiation of pure substrate did not cause the formation of particles.

RESULTS AND DISCUSSION

DLS studies of PVA solutions alone (Figure S1 in Supporting Information) showed a bimodal size distribution pointing to the

**Figure 2.** Example potentiometric titration data and ζ -potential of PVA-3250 (10 mM, in 0.02 NaCl).**Figure 3.** DLS data of the products of silicic acid condensation (10 mM, 10 days) at various pH values.

samples most likely including both single chains (5–20 nm) and aggregates (50–300 nm). This was confirmed by the SLS measurements, Table 1. DP values exceeded the DP of PVFA precursors, especially for the low molecular weight fractions. The presence of associates was observed at pH 5.5–10, and the aggregates are more pronounced at high pH values. Potentiometric titration and zeta potential measurements of the polymers alone (Figure 2) show an increase of protonation from 0 at pH 10 to 30% at pH 5.5. ζ -Potential remains positive at high pH, probably due to sorption of Na^+ ions onto the polymer chains.

Condensation of sodium silicate in the presence of the polymers was explored over a range of pH values from about 5.5 (the pH value suggested to occur in silica deposition vesicles of diatom algae²⁷) through neutral pH, where silica condensation is usually very fast, through to pH 10, which is just at the $\text{p}K_a$ value for orthosilicic acid.²³ Condensation of free $\text{Si}(\text{OH})_4$ (Figure 3) results in bimodal distributed particles at pH 8–10, with particles >100 nm. At $\text{pH} \leq 7$, small particles <30 nm were observed. Aggregation at $\text{pH} > 7$ to give ~ 100 nm silica particles had been described previously,^{23,28} but at $\text{pH} \leq 7$, condensation of primary particles usually results in three-dimensional gel networks. In this study, no gelation or precipitation was observed over two weeks at $\text{pH} \leq 7$, possibly due to the low silicon concentration (10 mM) used. This behavior (the formation of stable “soluble” particles containing silica) was not observed if the molar ratio of $[\text{Na}_2\text{SiO}_3]/[\text{PVA}]$ was increased to 1.5:1 and above, with precipitates being observed for the pH range 4–9.5.

The effect of the presence of PVA polymers on the rate of condensation of silicic acid was checked using the colorimetric molybdenum blue method²³ (example data is shown in Figure 4). Measurement of the concentration of noncondensed species (monomers and dimers) and subsequent data treatment²⁴ allows the extent of condensation to be measured as well as rate constants for the very early stages of condensation (formation of the smallest oligomers of silicic acid) to be calculated. Use of this method in the $\text{Si}(\text{OH})_4$ –PVA system showed that the

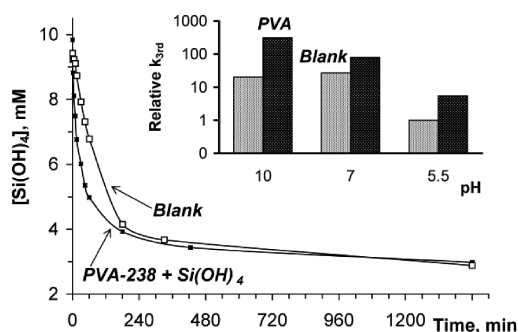


Figure 4. Example data set showing the effect of the PVA on condensation of silicic acid at pH 10 and the k_{third} for the $\text{Si}(\text{OH})_4$ at various pH. All rate constants are relative to the blank at pH 5.5. $[\text{PVA}] = [\text{Si}(\text{OH})_4] = 10 \text{ mM}$ in the initial solutions.

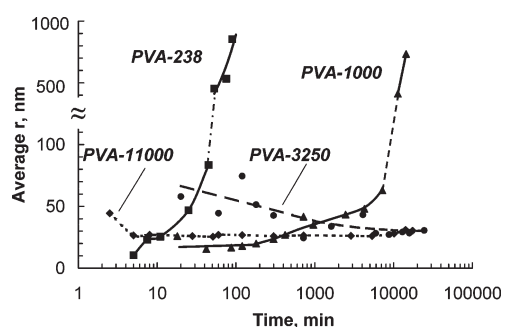


Figure 5. DLS data of the system PVA–silicic acid at pH 10. $[\text{PVA}] = [\text{Si}(\text{OH})_4] = 10 \text{ mM}$.

presence of PVA, at all pH values explored, increased the rate of condensation, the effect being most marked at the highest pH, with the effect of the polymer being clearly seen during the first few hours of the reaction. The equilibrium concentration of silicic acid was 2.8–3 mM after 2 days for all pH values, including blank experiments without PVA (Figure 4).

Analysis of polymer/silicic acid composite samples by light scattering methods showed a strong effect of polymer size on particle size, particularly for experiments performed at pH 10 (Figures 5 and 6). In the presence of low molecular weight fractions, there was a gradual increase in size of the particles in solution followed by fast aggregation with an appearance of an additional peak in the last stage (Figure 6a) and precipitation after 75 min and 10 days for PVA-238 and PVA-1000, respectively. Higher molecular weight fractions gave solutions of $\approx 30 \text{ nm}$ particles that were stable for more than two weeks. At initial time points (first days), large aggregates, several hundreds of nanometers in diameter, were also visible (Figure 6b), but with time (about a week), they gradually turned into stable nanoparticles that also remained stable over extended periods of time.

Condensation at pH 5.5 and 7 did not give precipitates with any PVA fraction. The detailed DLS study showed transitions from a bimodal to unimodal distribution of sizes during the first hours of reaction, as was observed above for the PVA-3250 polymers at pH 10. The resulting particles were stable for more than 10 days. Hydrodynamic radius of the particles increases drastically at pH 5.5 (Table 2).

The stable particles formed from silicic acid and PVA were studied with multiangle DLS and SLS (Table 3), which allowed us to obtain more realistic r_h values by extrapolation of the data to

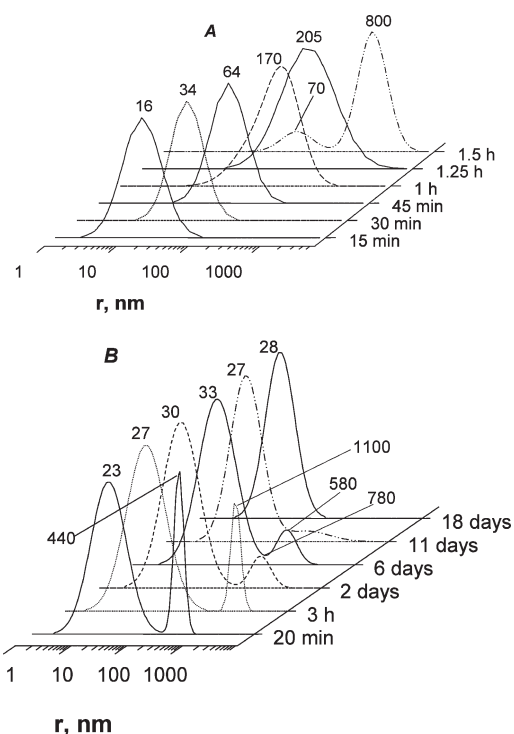


Figure 6. Size distribution of the particles formed on condensation of silicic acid in the presence of PVA-238 (A) and PVA-3250 (B) at pH 10.

Table 2. Hydrodynamic Radius (nm) of the Particles Formed after 10 Days Condensation of 10 mM Silicic Acid in the Presence of 10 mM PVA^a

pH	DP of PVA			
	238	1000	3250	11000
5.5	47	54	96	48
7	17	28	28	29
10	precipitate		33	29

^a Obtained by DLS, 173°, 633 nm scattering.

Table 3. Multiangle DLS and SLS Data of PVA–Silicic Acid Nanoparticles

DP	pH	r_g , nm	r_h , nm	r_g/r_h
11000	5.5	22.2	101.0	0.22
11000	7.0	26.5	52.9	0.50
11000	10.0	30.0	79.5	0.38
238	7.0	23.0	22.2	1.03
1000 ^a	10.0	23.8	23.8	1.00

^a After 72 h of the reaction, precipitation was observed to begin after 10 days.

0° scattering angle and also to measure r_g . The r_g/r_h ratios vary mostly with DP rather than pH: for high molecular weight samples, the values being those expected for microgels (0.3–0.6), and at short polymer chain length, the values are near 1 as appropriate for dendrimers and hyperbranched or star polymers. These values are also similar to values found for core–shell systems.²⁹ ζ -Potential measurements of these

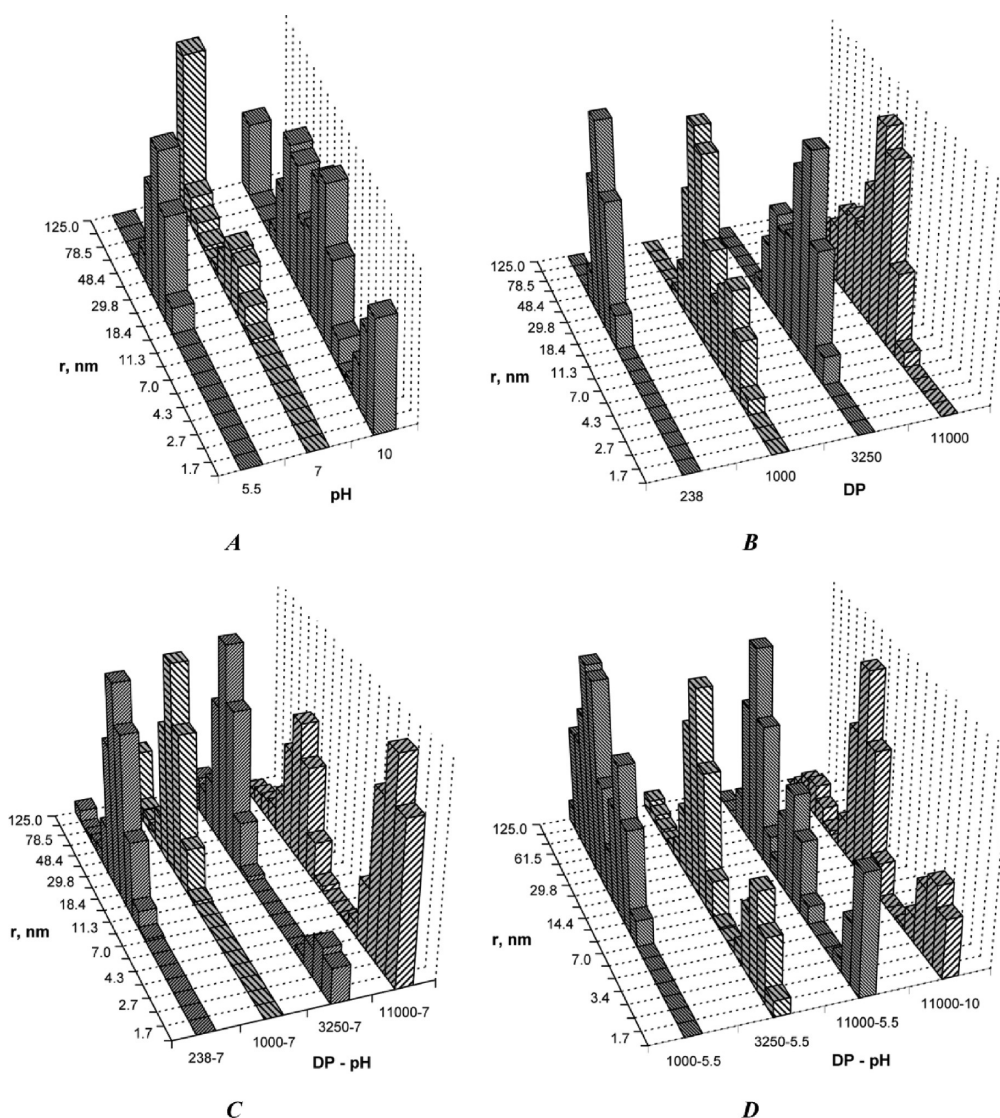


Figure 7. Laser ablation data for silica particles obtained without PVA (A), the studied solutions were prepared similar to the data presented in Figure 4), PVA samples of various DP (B), and composite nanoparticles (C, D). The polymer fractions used and the pH of the initial sample are indicated on the individual plots.

particles were positive, but accurate determinations were not possible because of changes in the particle size during measurements. The instability/destruction of composite nanoparticles under the action of an electric field points to their construction from oppositely charged components: negatively charged poly-(silicic acid) and positively charged PVA chains.

Laser ablation experiments were performed on PVA fractions, silica, and composite particles containing silica and PVA, with comparative samples to those used for the SLS/DLS experiments being freeze-dried onto aluminum foils for analysis. There was generally good agreement between the general trends observed by light scattering and analysis involving laser ablation (Figure 7). For the blank silica system (Figure 7A), all samples contain ablated particles close to that found in solution by DLS. In addition, at pH 10, small (<5 nm in diameter) particles were also detected (for explanation see below), and at pH 7, large particles (ca. 125 nm in diameter) not observed by DLS (Figure 3) were detected, suggesting that further condensation of silica particles with active silanol groups (pK_a of polymeric silicic acid is $\sim 6-7$)

occurred during sample preparation. The ablation products of PVA (Figure 7B) consist of two types of particles: relatively small (5–15 nm) and large (20–60 nm) particles. The PVA-11000 fraction gives mainly small particles and PVA-238 gives mainly large ones. Taking into account the DLS data, the small particles can be attributed to individual molecules and the large particles can be attributed to aggregates that are less common for PVA-11000. A comparison of the absolute particle sizes of PVA molecules from ablation and light scattering is not currently possible due to the high dependence of the size of flexible macromolecules in water on pH, concentration, and ionic strength.

The ablation data for composite nanoparticles (Figure 7C,D) generally show good agreement with what would be expected from the DLS/SLS data but also contain smaller (ca. 3–6 nm diameter) particles that are most significant for composites prepared in the presence of the high molecular weight PVA. These particles are absent in ablation spectra of PVA and can be possibly attributed to silica from the core of the composite particles. Assuming the density of silica as 2.2, the conversion of

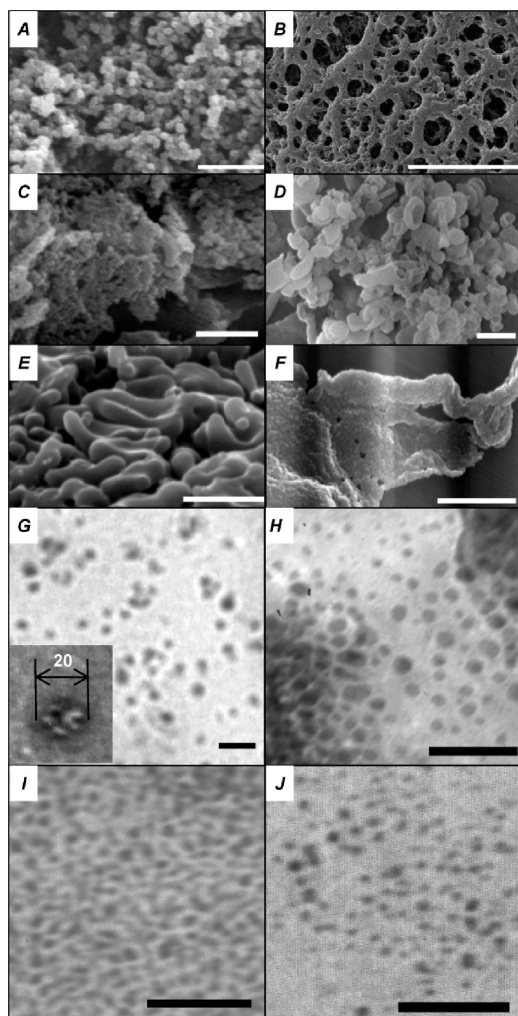


Figure 8. SEM (A–F) and TEM (G–J) images of composite precipitates (A) and freeze-dried solutions (B–J) with PVA-238 (A, D, G), PVA-1000 (E), 3250 (B), and 11000 (C, F, H–J). pH = 10 (A–C, H), 7 (D–G, I), and 5.5 (J). [PVA] = [Si(OH)₄] = 10 mM. Scale bar 1 μm (A, C–F), 10 μm (B), and 50 nm (G–J).

silicic acid as 70% (as measured from the molybdenum blue colorimetric analysis described earlier), and the diameter of silica nanoparticles as about 5 nm, we can calculate that the composite particles formed in the presence of PVA-11000 must contain 5–6 such silica nanoparticles. Taking into account the hydrodynamic radius of PVA-11000 (Table 1) and composites formed from it (Table 2) this seems reasonable. Samples based on low molecular weight polymer fractions do not show the small particles, suggesting that if such particles were present their size would have to be below the detection limit of the instrument.

Electron microscopy was used to confirm the size and the nature of the composite particles formed, Figure 8, and FTIR spectroscopy, Figure 9, was used to confirm the nature of bonding interactions between the polymer and the inorganic phase. Example SEM data (Figure 8A) of the composite precipitate obtained from PVA-238 at pH 10 show ≈ 100 nm particles, which were formed at the beginning of the fast aggregation stage after about 90 min of reaction, Figure 5. Drying of the soluble nanoparticles is accompanied by the formation of net-like structures at pH 10 (Figure 8B) or smoothed submicrometer particles

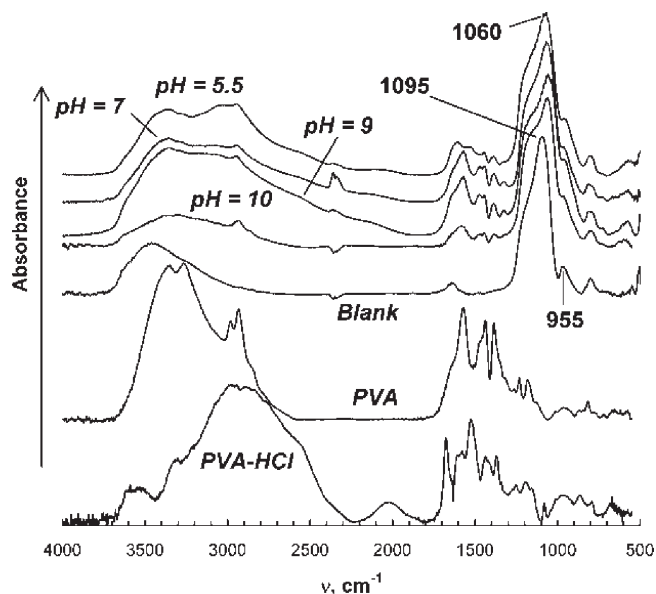


Figure 9. FTIR spectra of composite precipitates obtained for the system PVA-1000–Si(OH)₄ at various pH. [PVA] = 10 mM, [Si(OH)₄] = 10 mM (pH = 10), and 15 mM (pH = 5.5–9). Blank, silica obtained by precipitation from 50 mM sodium silicate at pH 7; PVA-HCl, salt obtained in excess of HCl.

at pH 7 (Figure 8D,E). A high molecular PVA sample gives (Figure 8C,F) aggregated <100 nm particles. In all cases, increasing the silicic acid to PVA ratio content in this system gives rise to large particles of indeterminate form, data not shown. TEM images (Figure 8G–J) contain electron-dense particles 5–30 nm in diameter, which evidently correspond to silica nanoparticles.

IR spectra of the composite precipitates (Figure 9) show a shift of the antisymmetric Si–O–Si stretching band from 1095 to 1060 cm^{-1} in the presence of PVA. Absorbance at 2000–2700 cm^{-1} can be attributed to protonated PVA units, providing evidence of ionic interactions between the polymer and inorganic components in the composite particles. In addition, an increase in relative intensity of the band at about 955 cm^{-1} suggests that the silica formed in the presence of PVA contains more silanol groups than the silica material prepared in the absence of the polymer. These phenomena were observed at pH 5.5–10, independently of the molecular weight of PVA. In the case of pH values below 10, 50% excess of silicic acid was used to obtain the precipitates because at equimolar PVA–silicic acid ratio the solutions are stable at pH 5.5–9.

A detailed exploration of the PVA–silicic acid reaction system by a number of experimental techniques has shown that condensation of silicic acid in the presence of PVA results in the formation of stable composite nanoparticles about 35–200 nm in diameter. However, questions arise in connection with the nature and properties of these particles as well as to how they are formed and stabilized.

Silica nanoparticles can react with polymeric bases and cations via surface silanol groups.^{30–32} This reaction obeys the laws of cooperative interpolymer reactions and gives immediate precipitation or stable solutions depending on the nature and chain length of the organic polymer, pH, ionic strength, and so on. In the case of the PVA–Si(OH)₄ system, condensation proceeds over hours (sometimes days) after starting the reaction. The composites contain considerably more silanol groups than for

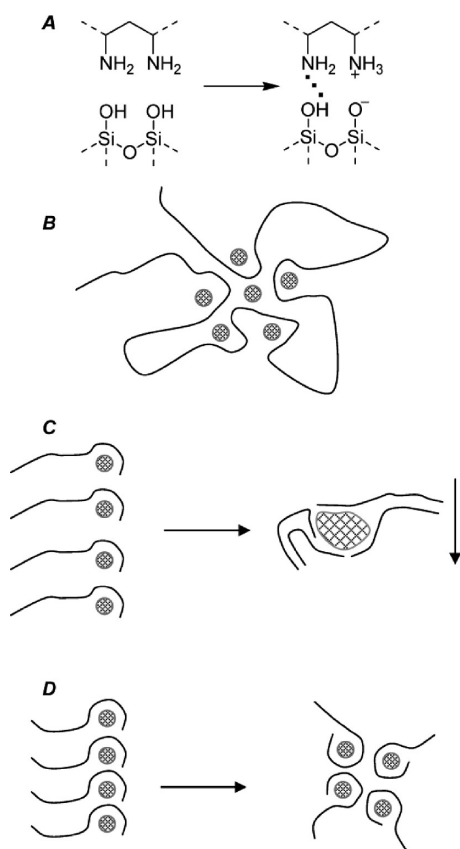


Figure 10. Scheme of interactions between condensed silicic acid and PVA chains (A) and structures of composite products formed with long-chain PVA macromolecules (B) and short chain PVA at pH 10 (C) and at pH 5–7 (D).

silica obtained without PVA (Figure 9, band at 955 cm^{-1}). We propose the following reaction sequence:

At the very beginning of the condensation process, the reaction solution contains a preponderance of $\text{Si}(\text{OH})_4$ molecules and certainly dimers and trimers that are able to interact with PVA chains by ionic and hydrogen bonds (Figure 10A).

Such interactions increase the concentration of $\text{Si}-\text{O}^-$ species that are the most active in reaction with weakly acidic monomeric silicic acid²³ with condensation proceeding by addition of uncharged $\text{Si}(\text{OH})_4$ to silanol anions in the growing composite nanoparticles. This process explains the observed acceleration of condensation (Figure 4) and continues until the equilibrium concentration of silicic acid in solution is reached.

The growth of silica particles is accompanied by strong cooperative interaction with PVA chains. Taking into account that the surface area per silanol group is $\approx 0.2\text{ nm}^2$,³² we can calculate that a silica particle of 1–2 nm in diameter contains 15–60 $\text{Si}-\text{OH}$ groups, which is enough for this interaction.

The ability of PVA to interact with silica particles depends on pH. At pH 10, the degree of protonation of PVA is very low and silanol groups are mostly ionized ($\text{p}K_a = 6-7$ ²³). The weakened interaction between a polymeric amine and silica sol at pH 9 comparing with pH 7 had been described earlier.³¹ Thus, the PVA–silica complex at pH 10 contains long PVA loops and tails. In the case of long-chain molecules, the macromolecular chain length is enough for complexing with a silica particle (or several particles), as shown in Figure 10B.

The complex obtained is relatively stable due to the protective action of the organic polymer on active silica groups. Short PVA chains are not able to encapsulate the whole silica nanoparticle at pH 10, so that further condensation proceeds with the non-charged PVA tails not being able to stabilize large silica particles in solution (Figure 10C).

At pH 5–7, PVA is partially protonated (Figure 2) and silica particles have sufficient $\text{Si}-\text{OH}$ and $\text{Si}-\text{O}^-$ groups for strong interaction with PVA by ionic and hydrogen bonds. The structure of the products from long-chain PVA is expected to be similar to that observed at pH 10. Short-chain polymers give rise to stable nanoparticles at these pH values, and their size (Table 2) points to the presence of several PVA macromolecules associated with an individual particle (Figure 10D). An increase of DP up to 11000 results in the formation of monomacromolecular based particles, and we observe a decrease of r_h (Table 2), especially at pH 5.5, where high PVA protonation and low silica ionization decreases PVA–silica interactions compared to the behavior observed at pH 7.

The composite nanoparticles formed in the presence of long and short PVA differ in r_g/r_h ratios (Table 3). The values correspond to core–shell structures, but materials formed in the presence of PVA-11000 give particles with lower r_g/r_h , suggesting that the particles contain a dense core surrounded with a large shell formed from a swelled polymeric chain. The more dense core with high molecular PVA is possibly explained by a concentration of all of the silica nanoparticles in a small area of the PVA chain, similar to that observed for metal–polymer complexes.^{33,34} This concentration may result in further condensing of the primary silica nanoparticles, giving rise to a dense core. Low molecular PVA forms composite particles as associates of several individual PVA–silica particles and the product also has a core–shell structure, but the core contains more PVA fragments that decrease its density and increase r_g/r_h ratio. The difference between silica particles formed with PVA-238 and PVA-11000 is evident from TEM data (Figure 8G–J): small particles being formed in the presence of PVA-11000 and larger aggregates up to 30 nm in diameter being formed in the presence of PVA-238.

We propose PVA as a simple model of polyamine-containing proteins in diatom algae. These proteins (silaffins) are associated with biosilica,^{11–14} but their role in the building of silica valves is not fully known.³⁵ Elemental analysis of diatom frustules showed low levels of organic matter in diatom frustules, which contradicts the hypothesis^{6,12} of the matrix role of silaffins in the formation of fine species-specific structures of frustules. Special silicon transport vesicles (STVs) have also been identified in the cytoplasm of diatoms that are proposed to be important in biosilica formation.³ The STVs are 20–50 nm particles that do not contain any electron-dense silica and so their existence is still debatable.¹⁰ However, in this contribution, we have shown that polymeric amines are able to stabilize condensed silicic acid in the formation of composite nanoparticles whose size is comparable with the hypothetical STVs. “Silicon” is captured within these particles in the form of small primary heavily hydroxylated particles, which are hardly detectable by microscopy of the natural samples but which we propose could be readily transported within an organism and be readily depolymerized (if required) at the point of use owing to the extremely high level of hydroxylation associated with the silicified component of the particles. These polymeric amines also accelerate the initial stage of condensation of $\text{Si}(\text{OH})_4$, which could be

Table 4. Particle Size and ζ -Potential of Composite Nanoparticles Obtained by Condensation of Silicic Acid (10 mM) in the Presence of VI-AA Copolymers (10 mM)

VI in copolymer, mol %	pH	r_h , nm	ζ -potential, mV
44	7	68	-39.4
69	7	66	-22.6
69	8	60	-30.8
85	8	27	-10.7

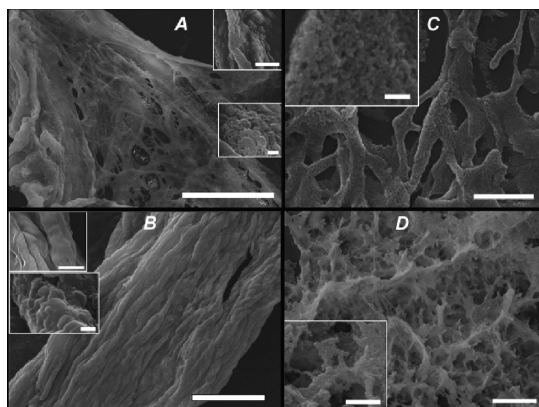


Figure 11. SEM images of precipitates obtained by mixing solutions with composite polymer-poly(silicic acid) nanoparticles. PVA-11000 and VI-AA copolymers (44 (A), 69 (B, D), and 85 (C) mol % VI in copolymer) were used as the organic macromolecules. Initial polymers and sodium silicate concentration: 10 mM, pH 7 (A, B) and 8 (C, D); Scale bar: 50 μm (A, B), 10 μm (A, top insertion), 5 μm (C, D and top insertion in B), and 0.5 μm (A and B, bottom insertions, C and D insertions).

used to facilitate the capture of silicic acid from the environment. From the results of this and other studies,^{7,20} the most probable form of silicic acid in the cytoplasm of diatoms will be core-shell complexes of primary silica particles with biogenic polymeric amines such as silaffins or components thereof.

Composite nanoparticles obtained in this work could be considered as new biomimetic precursors for the synthesis of silica structures under moderate conditions. The list of precursors available for the synthesis of silica-based materials from a solution environment now include sodium silicate, organic derivatives of silicic acid (tetraethylorthosilicate, sodium catecholate, etc.), and silica nanoparticles obtained by sol-gel methods.²⁸ The problems associated with the use of these precursors include fast, unregulated condensation of $\text{Si}(\text{OH})_4$ in the case of inorganic silicates, the requirement for hydrolysis, complications in mechanistic understanding, and the presence of residual unhydrolyzed organic moieties in the final material for syntheses involving organic ethers, and when silica nanoparticles are used, the inherent stability of the particles themselves restricts possibilities to synthesize low-dimensional nanostructures.

In contrast, core-shell composite nanoparticles as described in this paper are obtained from water, and contain silica nanoparticles surrounded by organic polymer, which provides compatibility with other polymers and may enable the design of more complicated structures using polymer-polymer interactions. As an example, recently we have shown the formation of composite nanoparticles during condensation of silicic acid in the

presence of poly(1-vinylimidazole).^{7,17} Additionally, copolymers of 1-vinylimidazole with acrylic acid (VI-AA) are also able to control silicic acid condensation and to give composite nanoparticles up to 56% acidic units.³⁶ These nanoparticles are negatively charged (Table 4) and were expected to interact with the positively charged PVA-based particles. Recently,³⁷ the importance of oppositely charged polymeric matrices for the formation of ordered organo-silica structures in living organisms has been demonstrated.

Solutions containing composite nanoparticles of opposite charge interact giving precipitates, often with an interesting fibrous shape (Figure 11). Products obtained at pH 8 (Figure 11C,D) consist of small (<100 nm) particles, and the fibrous structures at pH 7 contain large smoothed fragments admixed with small particles. These materials contain 40–50% of SiO_2 (according to molybdate colorimetric analysis) and are a promising type of composite³⁸ that do not require organic solvents and expensive and toxic silica precursors for their formation.

CONCLUSIONS

We have shown that condensation of silicic acid in the presence of poly(vinylamine) chains results in soluble nanoparticles or composite precipitates depending on DP of the organic polymer and pH. The nanoparticles in solution have core-shell like structures with a dense silica core in the case of high-molecular weight polymers. Composite particles based on polymers with a DP below 1000 are associates of several polymer-silica nanoparticles. We consider these polymer-poly(silicic acid) nanoparticles to be both a new silica precursor for the design of composite materials and to serve as a model for the storage of active silicic acid for use in silicifying organisms such as diatom algae.

ASSOCIATED CONTENT

S Supporting Information. Examples of DLS experimental data and calculated values; DLS data of 10 mM solutions of PVA fractions of various DP and pH values. This material is available free of charge via the Internet at <http://pubs.acs.org>.

AUTHOR INFORMATION

Corresponding Author

*E-mail: annenkov@lin.irk.ru; annenkov@yahoo.com.

ACKNOWLEDGMENT

We acknowledge support of an INTAS-SB RAS grant (#06-1000013-8569). V.V.A. and A.K.P. also acknowledge support from the Siberian Branch of the Russian Academy of Sciences (Project #39). We are thankful to Prof. V. A. Umanets (Russian State University of Physical Education, Sport and Tourism, Irkutsk division) for assistance with the TEM study.

REFERENCES

- Hildebrand, M. Silicic acid transport and its control during cell wall silicification in diatoms. In *Biomimetalization: From Biology to Biotechnology and Medical Application*; Baeuerlein, E., Ed.; Wiley-VCH: Weinheim, 2000; pp 171–188.
- Kinrade, S. D.; Gillson, A. M. E.; Knight, C. T. *J. Chem. Soc., Dalton Trans.* **2002**, 3, 307–309.
- Schmid, A.-M.; Schultz, D. *Protoplasma* **1979**, *100*, 267–288.

- (4) Parkinson, J.; Brechet, Y.; Gordon, R. *Biochim. Biophys. Acta* **1999**, *1452*, 89–102.
- (5) Perry, C. C. *Rev. Mineral. Geochem.* **2003**, *54*, 291–327.
- (6) Sumper, M. *Angew. Chem., Int. Ed.* **2004**, *116*, 2301–2304.
- (7) Annenkov, V. V.; Danilovtseva, E. N.; Likhoshway, Y. V.; Patwardhan, S. V.; Perry, C. C. *J. Mater. Chem.* **2008**, *18*, 553–559.
- (8) Bertermann, R.; Kröger, N.; Tacke, R. *Anal. Bioanal. Chem.* **2003**, *375*, 630–634.
- (9) Gröger, C.; Sumper, M.; Brunner, E. *J. Struct. Biol.* **2008**, *161*, 55–63.
- (10) Hildebrand, M.; Wetherbee, R. Components and control of silicification in diatoms. In *Progress in Molecular and Subcellular Biology*; Müller, W. E. G., Ed.; Springer-Verlag: New York, 2002; Vol. 33, pp 11–58.
- (11) Kröger, N.; Deutzmann, R.; Sumper, M. *Science* **1999**, *286*, 1129–1132.
- (12) Sumper, M.; Kröger, N. *J. Mater. Chem.* **2004**, *14*, 2059–2065.
- (13) Matsunaga, S.; Sakai, R.; Jimbo, M.; Kamiya, H. *ChemBioChem* **2007**, *8*, 1729–1735.
- (14) Sumper, M.; Brunner, E.; Lehmann, G. *FEBS Lett.* **2005**, *579*, 3765–3769.
- (15) Bridoux, M. C.; Ingalls, A. E. *Geochim. Cosmochim. Acta* **2010**, *74*, 4044–4057.
- (16) Kröger, N.; Sandhage, K. H. *MRS Bull.* **2010**, *35*, 122–126.
- (17) Annenkov, V. V.; Danilovtseva, E. N.; Filina, E. A.; Likhoshway, Y. V. *J. Polym. Sci., Part A: Polym. Chem.* **2006**, *44*, 820–827.
- (18) Pavlov, G. M.; Korneeva, E. V.; Ebel, C.; Gavrilova, I. I.; Nesterova, N. A.; Panarin, E. F. *Polym. Sci., Ser. A* **2004**, *46*, 1063–1067.
- (19) Petrov, A. K.; Kozlov, A. S.; Malyshev, S. B.; Taraban, M. B.; Popik, V. M.; Scheglov, M. A.; Goriachkovskaya, T. N.; Peltek, S. E. *Nucl. Instrum. Methods Phys. Res., Sect. A* **2007**, *575*, 68–71.
- (20) Grachev, M. A.; Annenkov, V. V.; Likhoshway, Ye. V. *BioEssays* **2008**, *30*, 328–337.
- (21) Gu, L.; Zhu, S.; Hrymak, A. N. *J. Appl. Polym. Sci.* **2002**, *86*, 3412–3419.
- (22) Annenkov, V. V.; Danilovtseva, E. N.; Tenhu, H.; Aseyev, V.; Hirvonen, S.-P.; Mikhaleva, A. I. *Eur. Polym. J.* **2004**, *40*, 1027–1032.
- (23) Iler, R. *The Chemistry of Silica*; Wiley: New York, 1982.
- (24) Belton, D.; Paine, G.; Patwardhan, S. V.; Perry, C. C. *J. Mater. Chem.* **2004**, *14*, 1–12.
- (25) Ankilov, A.; Baklanov, A.; Colhoun, M.; Enderle, K.-H.; Gras, J.; Julanov, Yu.; Kaller, D.; Lindner, A.; Lushnikov, A. A.; Mavliev, R.; McGovern, F.; O'Connor, T. C.; Podzimek, J.; Preining, O.; Reischl, G. P.; Rudolf, R.; Sem, G. J.; Szymanski, W. W.; Vrtala, A. E.; Wagner, P. E.; Winklmayr, W.; Zagaynov, V. *Atmos. Res.* **2002**, *62*, 209–237.
- (26) Gavrilov, N. G.; Knyazev, B. A.; Kolobanov, E. I.; Kotenkov, V. V.; Kubarev, V. V.; Kulipanov, G. N.; Matveenko, A. N.; Medvedev, L. E.; Miginsky, S. V.; Mironenko, L. A.; Oreshkov, A. D.; Ovchar, V. K.; Popik, V. M.; Salikova, T. V.; Scheglov, M. A.; Serednyakov, S. S.; Shevchenko, O. A.; Skrinisky, A. N.; Tcheskidov, V. G.; Vinokurov, N. A. *Nucl. Instrum. Methods Phys. Res., Sect. A* **2007**, *575*, 54–57.
- (27) Vrieling, E. G.; Gieskes, W. W. C.; Beelen, T. P. M. *J. Phycol.* **1999**, *35*, 548–559.
- (28) Brinker, C. J.; Scherer, G. W. *Sol-Gel Science: The Physics and Chemistry of Sol-Gel Processing*; Academic Press: London, 1990.
- (29) Burchard, W. *Adv. Polym. Sci.* **1999**, *143*, 113–194.
- (30) Yermakova, L. N.; Aleksandrova, T. A.; Nuss, P. V.; Vasserman, A. M.; Kasaikin, V. A.; Zezin, A. B.; Kabanov, V. A. *Polym. Sci. U.S.S.R.* **1985**, *27*, 2073–2080.
- (31) Yermakova, L. N.; Nuss, P. V.; Kasaikin, V. A.; Zezin, A. B.; Kabanov, V. A. *Polym. Sci. U.S.S.R.* **1983**, *25*, 1605–1616.
- (32) Yermakova, L. N.; Frolov, Yu. G.; Kasaikin, V. A.; Zezin, A. B.; Kabanov, V. A. *Polym. Sci. U.S.S.R.* **1981**, *28*, 2529–2544.
- (33) Anufrieva, E. V.; Gromova, R. A.; Lushchik, V. B.; Nekrasova, T. N.; Krakovyak, M. G. *Vysokomol. Soedin., Ser. B* **1996**, *38*, 1614–1618.
- (34) Annenkov, V. V.; Kruglova, V. A.; Alsarsur, I. A.; Shevtsova, Zh. V.; Aprelkova, N. F.; Saraev, V. V. *Polym. Sci., Ser. B* **2002**, *44*, 12. P. 295–299.
- (35) Ingalls, A. E.; Whitehead, K.; Bridoux, M. C. *Geochim. Cosmochim. Acta* **2010**, *74*, 104–115.
- (36) Annenkov, V. V.; Danilovtseva, E. N.; Pal'shin, V. A.; Likhoshway, Y. V. *Adv. Sci. Lett.* **2011**, *4*, 616–621.
- (37) Scheffel, A.; Poulsen, N.; Shian, S.; Kröger, N. *Proc. Natl. Acad. Sci. U.S.A.* **2011**, *108*, 3175–3180.
- (38) Wilkes, C. L.; Wen, J. Organic-inorganic composites In *Polymeric Materials Encyclopedia*; Salamone, J. P., Ed.; CRC Press: Boca Raton, New York, London, Tokyo, 1996; pp 4782–4792.